Trans Indian Inst Met (2024) 77(9):2739–2750
https://doi.org/10.1007/s12666-024-03372-2

ORIGINAL ARTICLE

Microstructural, Mechanical and Tribological Behaviour of NiTi/SiC/ZrO_2 Reinforced Aluminium 6061 Hybrid MMCs

Saurabh Kumar Maurya[1] · **Chander Kant Susheel**[1] · **Alakesh Manna**[1]

Received: 24 January 2024 / Accepted: 23 May 2024 / Published online: 6 June 2024

Abstract Aluminium metal matrix composites (AMMCs) are replacing the monolithic alloys for advance engineering applications in industries. Present work appraised the use of fragmented aluminium with the reinforcement of SiC, ZrO_2 and NiTi mixture. Mechanical and microstructural properties of fabricated AMMCs were evaluated, and it was found that fabricated composites have finer grain structure compared to the base alloy. Tensile strength of base alloy was enhanced by 44.8% due to refinement of the grains, shear lag and bowing of dislocations. The maximum value of compressive strength, microhardness and impact strength was found in composite with 3wt% reinforcement of each of SiC, ZrO_2 and NiTi. The transformation of ductile to cleavage fracture was confirmed by fracture morphology. Tribological analysis reveals that the material loss due to wear and roughness of worn-out surfaces was decreased by the accumulation of reinforcement.

✉ Saurabh Kumar Maurya
skks.saurabh@gmail.com

[1] Department of Mechanical Engineering, Punjab Engineering College (DU), Chandigarh, India

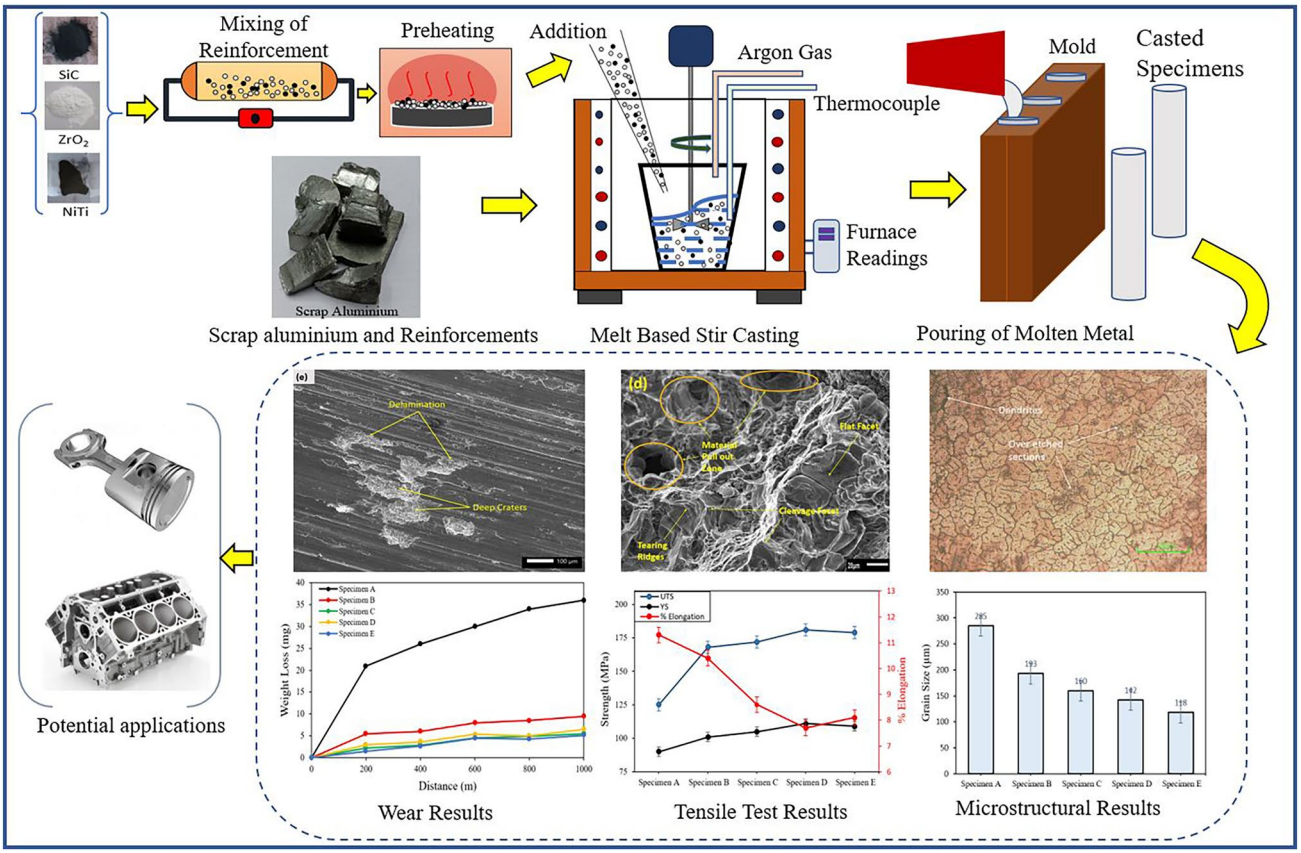

Keywords Hybrid AMMCs · Stir-casting · Microstructure · Fractography · Tribology

1 Introduction

Nowadays, materials required having good mechanical properties, light-weight, high ductility, corrosion and wear resistance for numerous engineering applications. Conventional monolithic materials have limitation of good combination of mechanical and tribological properties. To overcome these limitations and serve the latest demands, researchers are focused more on the development of metal matrix composites (MMCs). MMCs are becoming one of the best possible alternatives in several field like mechanical, structural and aeronautics due to its excellent mechanical, tribological and corrosion properties [1, 2].

These properties of any MMCs significantly depend on the casting technique utilised for fabrication, and from the experiments, stir-casting process was found most suitable for fabrication of aluminium metal matrix composites (AMMCs) due to its simplicity, lower cost and mass production capability [3]. However, these properties are also affected by the casting process parameters such as melting temperature, stirring speed, time, stirrer-shape, pouring temperature, and mould material. [4].

The mechanical properties of aluminium alloy increase with the weight percentage of SiCp reinforcement in the fabricated Al/SiC_p-MMC but at the same time impact toughness decreases [5]. The fabricated Al-6063-SiC_p-MMC utilising stir-casting technique improved the tensile strength, hardness and impact strength due to reduction in grain size and percentage elongation [6]. Reinforcement of 1.5wt%SiCp in AA365 showed comparatively higher tensile and compressive strength over other combination of wt% of SiC_p reinforcement [7]. Mechanical properties of Al6061/SiC_p-MMC were improved up to 3wt%SiC_p reinforcement [8]. Al7075/SiC_p-MMC (with 2wt%SiC_p) fabricated through ultrasonic cavitation-assisted stir-casting technique improved yield strength and wear resistance by 94.52 and 79.8%, respectively [9]. Effect of SiC_p in AA5083 has significant role in the increment of tensile strength, compressive strength, hardness and wear resistance [10]. Addition of ZrO_2 in AA6061/ZrO_2/Graphite-MMC increases the mechanical and tribological properties of fabricated-MMC over base alloy and AA6061/Graphite-MMC [11]. Mechanical properties of AA6082 were significantly improved by reinforcing ZrO_2 and coconut-shell. However, tensile strength of Al6082/ZrO_2/coconut-shell-MMC started decreasing with

ZrO_2 beyond 10wt% [12]. ZrO_2 reinforcement enhanced the mechanical, physical and tribological properties of AA6061 [13]. Al6061/ZrO_2-MMC with 3wt%ZrO_2 provides optimum mechanical properties, wear and corrosion resistance [14]. Hybrid Al/SiC/ZrO_2-MMC have enhanced hardness and wear resistance over Al/SiC and Al/ZrO_2-MMC [15]. Mechanical properties such as impact strength, tensile strength and hardness of A6082/SiC/ZrO_2-MMC were improved by 60%, 33%, and 17%, respectively, when compared to AA6082 [16]. Al-MMC with 3wt% of SiC/Graphite/ZrO_2 reinforcement resulted in optimum mechanical properties and corrosion resistance [17].

It was found that the yield strength, UTS and fatigue performance of AA1090 were boosted by reinforcing 10wt%NiTi, whereas percentage elongation was reduced [18]. The good bonding was found between AA1100 and $NiTi_p$ in friction stir processed AA1100/NiTi-MMC and improved mechanical properties by $NiTi_p$ reinforcement [19]. The presence of $NiTi_p$ improved the precipitation kinetics, damping capacity and microhardness of AA2124/NiTi-MMC [20]**.** Al6061/NiTi-MMCs with $NiTi_p$ (2–74 µm) have higher strength over $NiTi_p$ (150–178 µm), whereas comparatively higher ductility of the composites with $NiTi_p$ (150–178 µm) [21]. Fabricated Al-NiTi-SiC composite resulted in significant increment in hardness and compressive strength [22]. Fabricated AA1050/NiTi-MMC resulted in increment in the fracture toughness and UTS when

Table 1 Elemental composition of AA6061

Elements	Si	Mg	Mn	Cu	Ti	Fe	Zn	Cr	Al
wt%	0.71	0.80	0.17	0.26	0.13	0.55	0.21	0.05	Balance

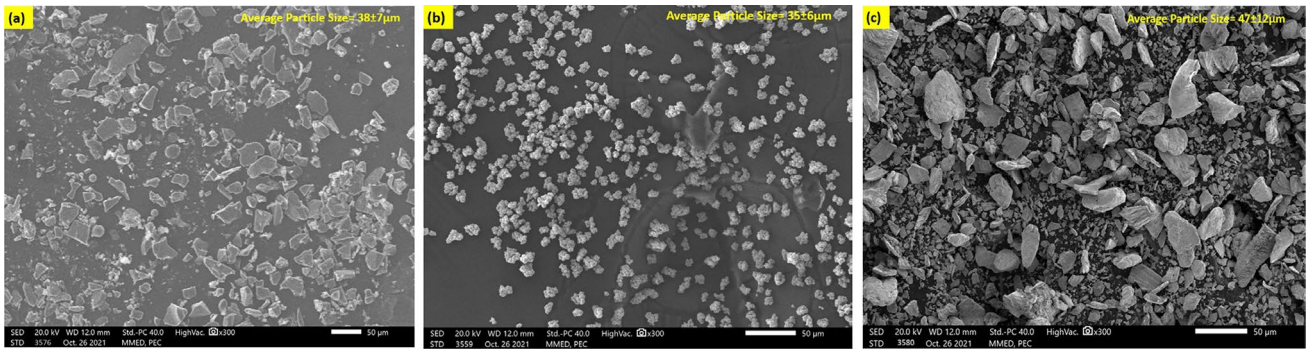

Fig. 1 SEM images of the reinforced particles **a** SiC; **b** ZrO_2; **c** NiTi

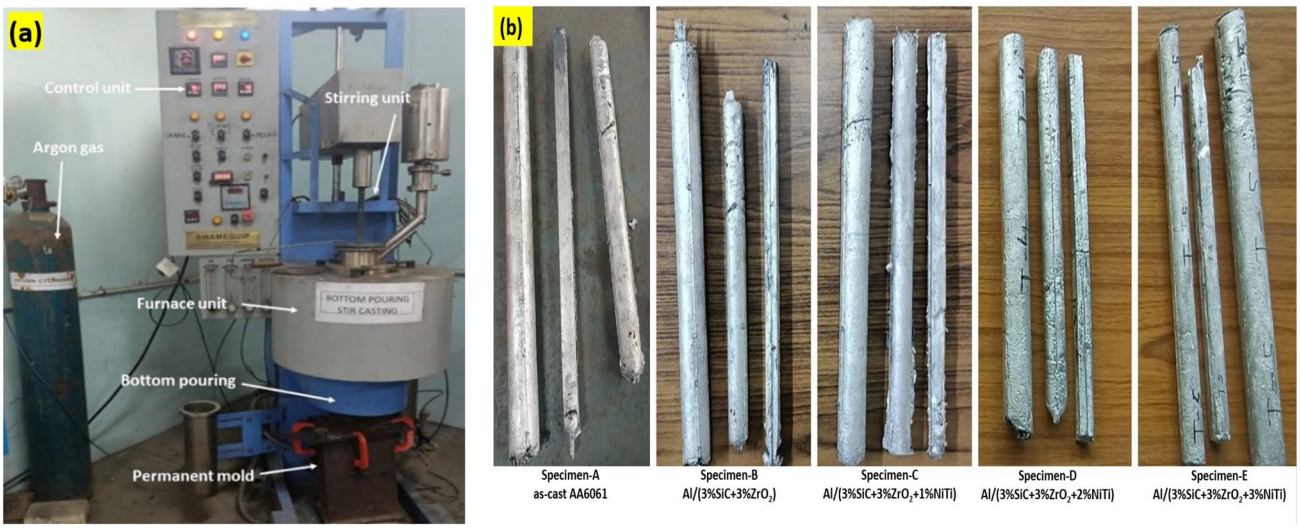

Fig. 2 **a** Stir-casting set-up; **b** different fabricated AMMC specimens

Table 2 Composition of the fabricated AMMC specimens

Fabricated specimens	Composition
A	as-cast AA6061
B	AA6061 + 3%SiC + 3%ZrO_2
C	AA6061 + 3%SiC + 3%ZrO_2 + 1%NiTi
D	AA6061 + 3%SiC + 3%ZrO_2 + 2%NiTi
E	AA6061 + 3%SiC + 3%ZrO_2 + 3%NiTi

compared to AA1050. The local internal stresses were also identified due to the shape memory effect of $NiTi_p$ [23].

From the literature review, it is found that, although the researchers have investigated the effect of reinforcement of SiC, ZrO_2 and NiTi on the fabricated MMCs, but the combined effect of reinforcement of these particles together on the microstructural, mechanical and tribological behaviour of fabricated hybrid AMMC is still missing. Therefore, in the present work, an attempt was made to fabricate a hybrid composite by diffusing together a unique mixture of SiC, ZrO_2 and NiTi particulates in AA6061 utilising stir-casting method and investigated the microstructure, mechanical and tribological behaviour of it. The fabricated MMCs can be used for different components used in automobile, airspace, marine and defence industry applications. They can also be used in the fabrication of different equipment's used in water treatments plants such as gates (sluice gates, weir gates, open channel gates, etc.), screening devices and stop-logs.

2 Materials and Methods

2.1 Matrix and Reinforcement

For the fabrication of Al/(SiC/ZrO_2/NiTi)-MMC, scrap of AA6061 was purchased from J.V. Mill & Hardware, Industrial Area Phase-II, Chandigarh-160002, whereas SiC, ZrO_2 and NiTi particulates were from Nanoshel, Dera Bassi, Punjab-140201. The elemental composition of AA6061 was measured by spark spectroscopy and is shown in Table 1. The average size of the reinforced SiC_p, ZrO_{2p} and $NiTi_p$ was 38 ± 7, 35 ± 6 and 47 ± 12 µm, respectively. Scanning electrode microscopic (SEM) images illustrate that the shape of SiC_p is thin and flat with sharp edges, ZrO_{2p} is granular with less size variation, and $NiTi_p$ is bumpy, (Fig. 1).

2.2 Fabrication of Hybrid Al/(SiC/ZrO_2/NiTi)-MMC

For the fabrication of Al/(SiC/ZrO_2/NiTi)-MMCs, stir-casting technique was used. AA6061 scrap was cut and washed with acetone for dirt removal. It melted in graphite crucible at 760 °C in argon gas atmosphere using resistance heating furnace. Preheated (at 350 °C) SiC_p, ZrO_{2p} and $NiTi_p$ were added to the melted aluminium and mixture was kept at 750 °C for 30 min. A stirrer (650 rpm) was applied for the proper mixing of reinforcement and molten matrix at 760 °C. Wettability between reinforcement and matrix was improved by the addition of 1wt%magnesium. Hexachloroethane (C_2Cl_6) was used for degassing the entire melt after 40 min. Post-removal of slag, mixture was emptied into preheated steel mould at 700 °C. For making a comparative study, base alloy was also casted. Figure 2 represents the casting set-up and different fabricated AMMC specimens, whereas Table 2 represents the composition of it.

2.3 Characterisation

For the characterisation, samples were extracted from the fabricated specimens. They were refined using emery paper followed by diamond paste (0.25 µm) on disc polishing. Further, high grade PFA cloth was used to accomplish glassy finish. At last, etching was performed by applying Keller's reagent. Optical images were taken to explain the metallographic characteristics. Vickers microhardness tester Model:HV-1000B was used to determine the microhardness by applying 500 g load for 10 s.

Samples for tensile, compression and impact test were prepared as per ASTM E8/E8M-16a, ASTM E9-19 and ASTM-E23 standards, respectively [24–26]. Instron™ Universal Testing Machine (100 KN) was used for tensile test with strain rate of 1×10^{-4} s^{-1}, whereas Charpy impact testing machine (22 kg hammer) was used for impact test. Wear tests were performed on pin-on-disc (made of EN 32,

Table 3 Mechanical test results for fabricated specimens

Properties	Fabricated Specimens				
	A	B	C	D	E
Ultimate tensile strength (MPa)	125 ± 3.5	168 ± 4.5	172 ± 4.0	181 ± 4.0	179 ± 4.5
0.2% offset yield strength (MPa)	90 ± 3.0	101 ± 3.5	105 ± 3.5	111 ± 3.0	109 ± 4.0
Elongation (%)	11.3 ± 0.5	10.4 ± 0.5	8.6 ± 0.4	7.7 ± 0.3	8.1 ± 0.4
Compressive strength (MPa)	283 ± 9	317 ± 12	331 ± 14	345 ± 12	363 ± 16
Microhardness (hv)	52 ± 3.5	69 ± 4.0	78 ± 4.5	84 ± 4.0	89 ± 3.5
Impact strength (joule)	16.6 ± 0.6	16.1 ± 0.5	18.3 ± 0.7	18.9 ± 0.6	19.0 ± 0.5

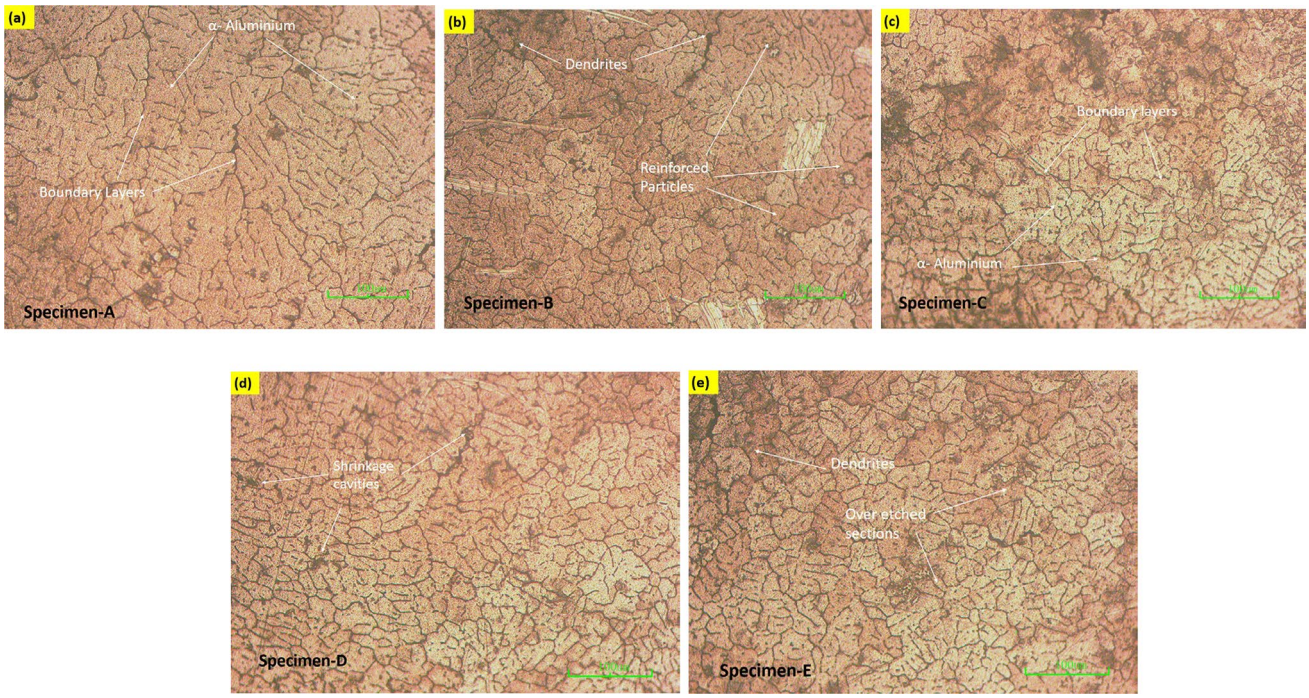

Fig. 3 Microstructural analysis of fabricated AMMCs specimens

hardness 62HRC) wear testing machine in dry sliding condition with 1 m/s velocity and 40N load. Sample of sizes 8 mm diameter and 30 mm length was extracted from the fabricated specimens for wear test. The samples were tested for total 1000 m distance, and wear loss was measured after every 200 m of sliding. Table 3 represents the results acquired from the mechanical tests.

3 Result and Discussion

A comparative study on microstructural, mechanical and tribological behaviour of the fabricated Al/SiC/ZrO_2/NiTi-MMC specimens was performed and analysed in the following subsections.

3.1 Microstructural Analysis

For demonstrating microstructural properties of fabricated AMMCs, optical micrographic images were used. Figure 3a shows the dendritic structure, elongated primary α-Al dendrites, irregular Al–Si eutectic segments in Specimen-A. It also discloses the existence of second phase Al(MgZn). Specimen-A shows uneven, harsh, and arbitrarily oriented grain structure. The measured average grain size of the specimens (A–E) is 285 ± 30, 193 ± 26, 160 ± 20, 142 ± 17 and 118 ± 14 µm, respectively. It is clear that average grain size of fabricated AMMC was decreased as the reinforced particle increased. It is because of reinforced particles limit the formation of grains. In composites, heterogeneous nucleation during solidification also causes the formation of smaller grains [7, 11, 27]. Furthermore, addition of NiTi allows higher resistance to grain formation, consequently finer grain structure is obtained [20]. There is 58% of grain refinement is resulted due to the combined effect of reinforcement of SiC, ZrO_2 and NiTi which is comparatively greater than the previously published research [6, 14, 18].

The presence of low porosities can be seen in the fabricated AMMCs. Degassing and casting of AMMCs in inert gas (argon) environment allow very less entrapment of atmospheric gases during casting. SEM images and EDS mapping of polished Specimen-E are shown in Fig. 4a–c. Figure 4a–b confirms the presence of web and foggy-shaped reinforced particles with random distribution in the matrix. Some particle rich and free portions can also be present due to dissimilar effect of vortex flow provided by stirrer and mechanical agitation. Clean particle–matrix interface can be observed from the SEM image (Fig. 4b). It helps in easy load transfer from matrix to reinforcement and, therefore, improves the load bearing capacity of the fabricated AMMCs. EDS mapping confirms the presence of all type of reinforcement in the fabricated AMMC (Fig. 4c).

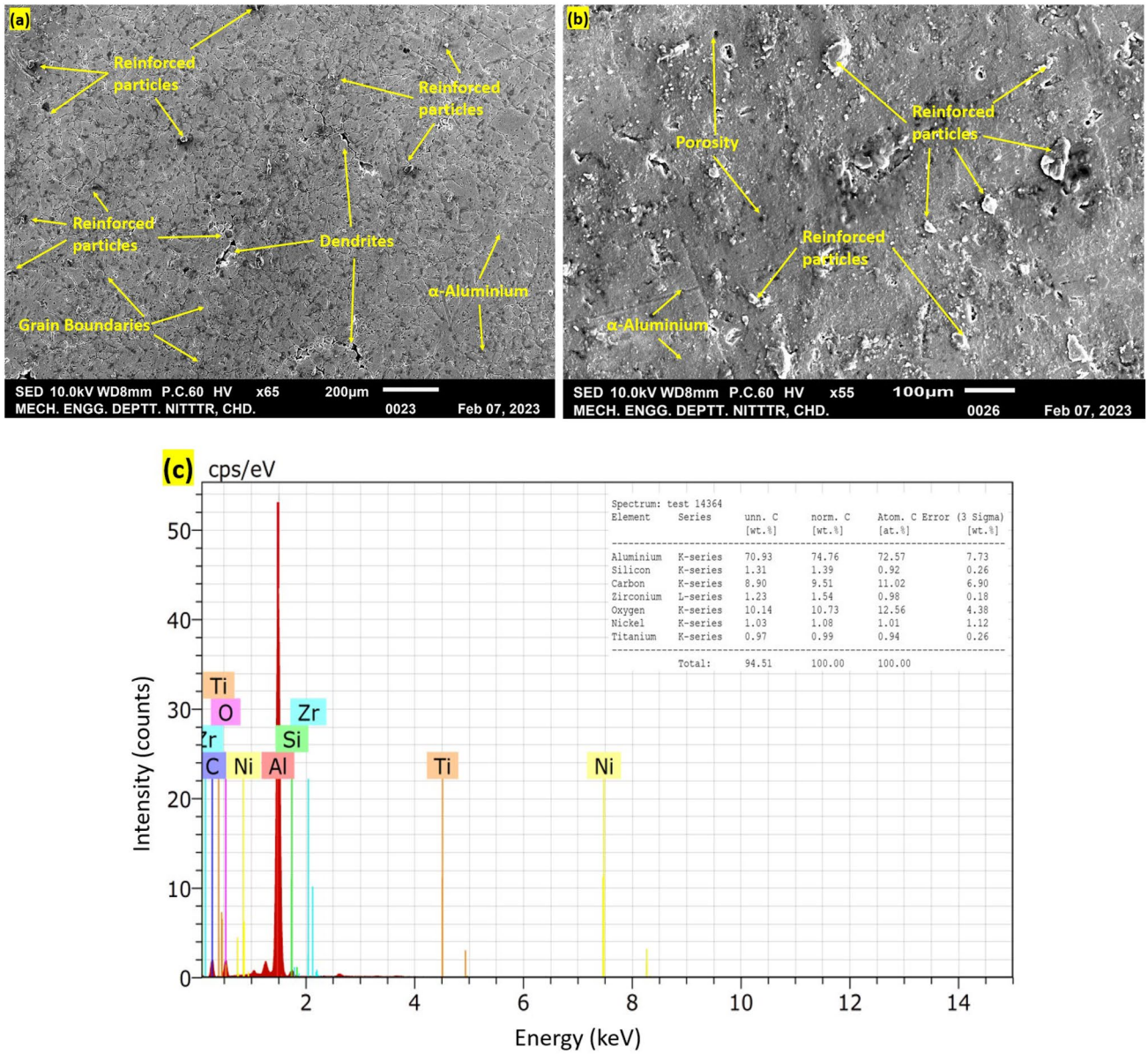

Fig. 4 **a**, **b** SEM image; **c** EDS mapping; of Specimen-E

3.2 Mechanical Properties

It can be supposed that the fabricated AMMC results in better mechanical behaviour when compared to the base alloy. Hence, in the present study, tensile, compressive, microhardness and impact test were carried out for investigating the mechanical behaviour of fabricated AMMCs under the influence of reinforcement. SEM images of tensile tested specimens were used to determine the mechanism of fracture involved.

3.2.1 Tensile Test and Fractography

Tensile strength plays a crucial role in the selection of material for the particular application. Uniaxial tensile tests were carried out on specimens, and results are shown in Fig. 5. It was found that as-cast AA6061 has lowest value of UTS, YS and highest % elongation, i.e. ~ 125 MPa, ~ 90 MPa and ~ 11.3%, respectively. However, fabricated AMMCs have higher UTS, YS and lower % elongation, compared to as-cast AA6061. AMMC Specimen-D (3wt%SiC, 3%wtZrO_2 and 2wt%NiTi) have maximum UTS and YS.

Tensile strength of any composite material is mainly decided by the grain size, numbers of dislocations,

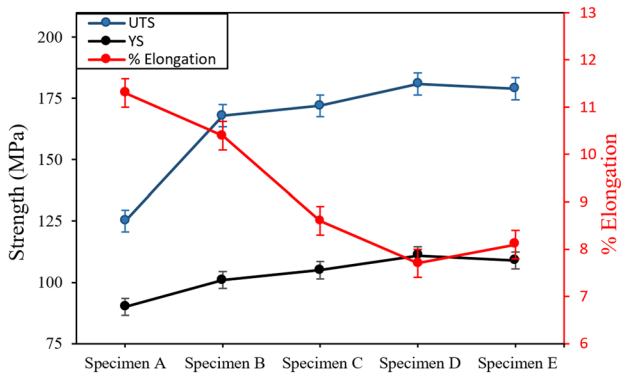

Fig. 5 Variation in the strength and % elongation of fabricated specimens

interfacial appearances, etc., and it can be improved by grain refinement, shear lag, matrix–reinforcement coefficient of expansion difference and dislocation bowing. Hall–Petch relation enlightened the effect of refinement of grain on improved strength [28]. In the composites, movement of dislocation is prohibited by uniformly distributed reinforced particles, which ultimately increases the strength of composites. Clean interface (Fig. 4) results more competent transfer of load from matrix to the reinforcement during tensile testing. Due to varying nature of matrix and reinforcement, additional dislocations were formed, acting as the obstacle for movement of other dislocations and increasing the tensile strength. Also, formation of micro-voids during casting decreases the ductility of the fabricated AMMCs and responsible for the crack initiation during tensile test. During tensile straining, existence of α-Al dendrites and coarse acicular Si particles acts as the stress concentration sites and lowers the ductility. Stress concentration also results the crack nucleation and

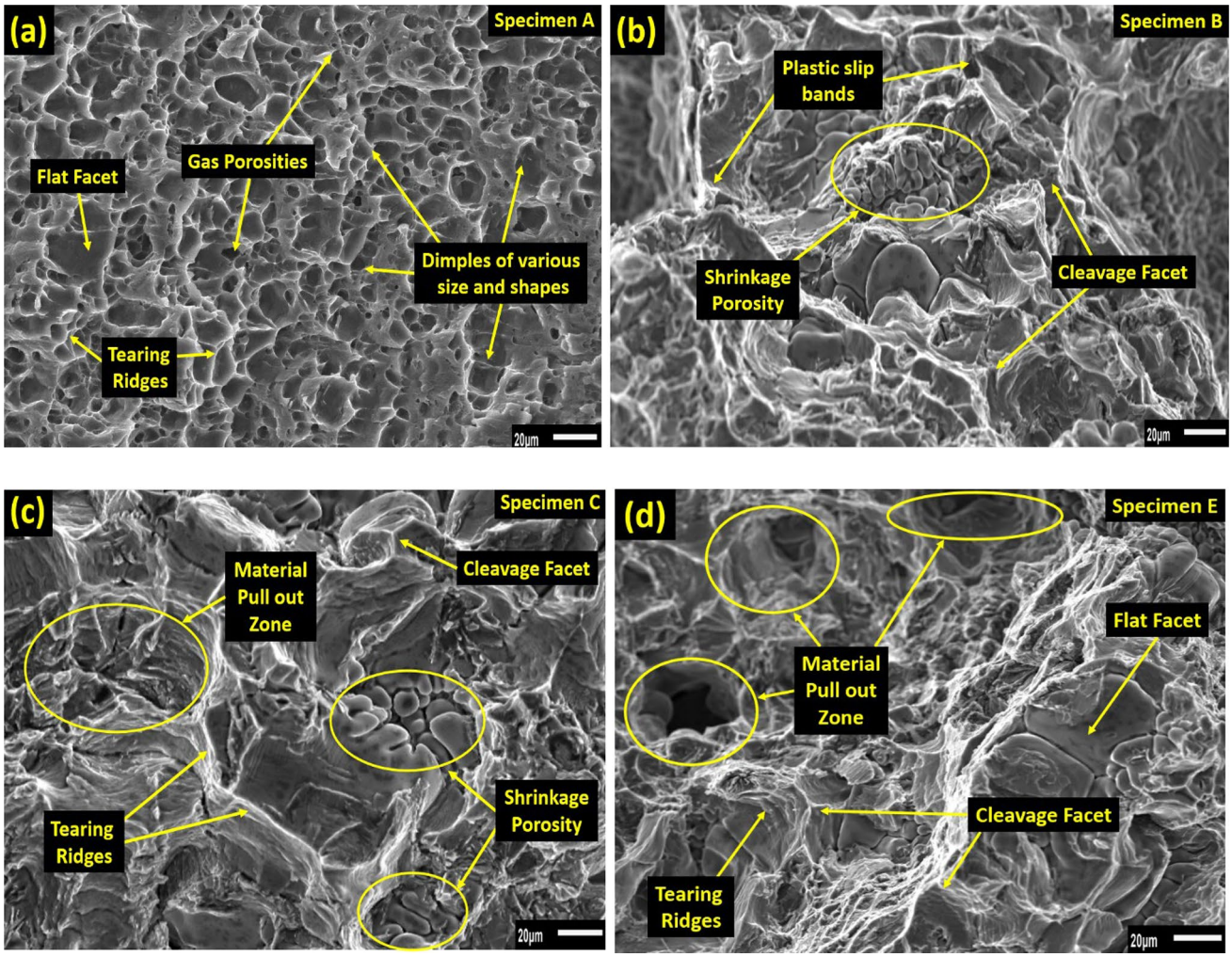

Fig. 6 SEM of fractured surface of fabricated specimens

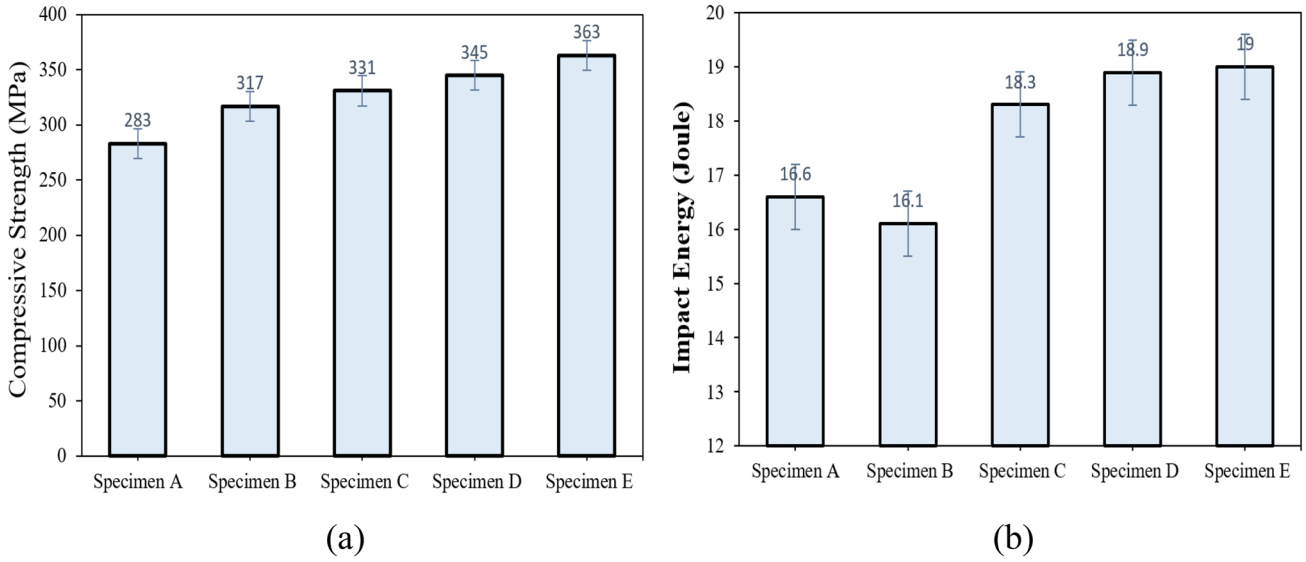

Fig. 7 **a** Compressive strength, **b** impact energy of fabricated specimens

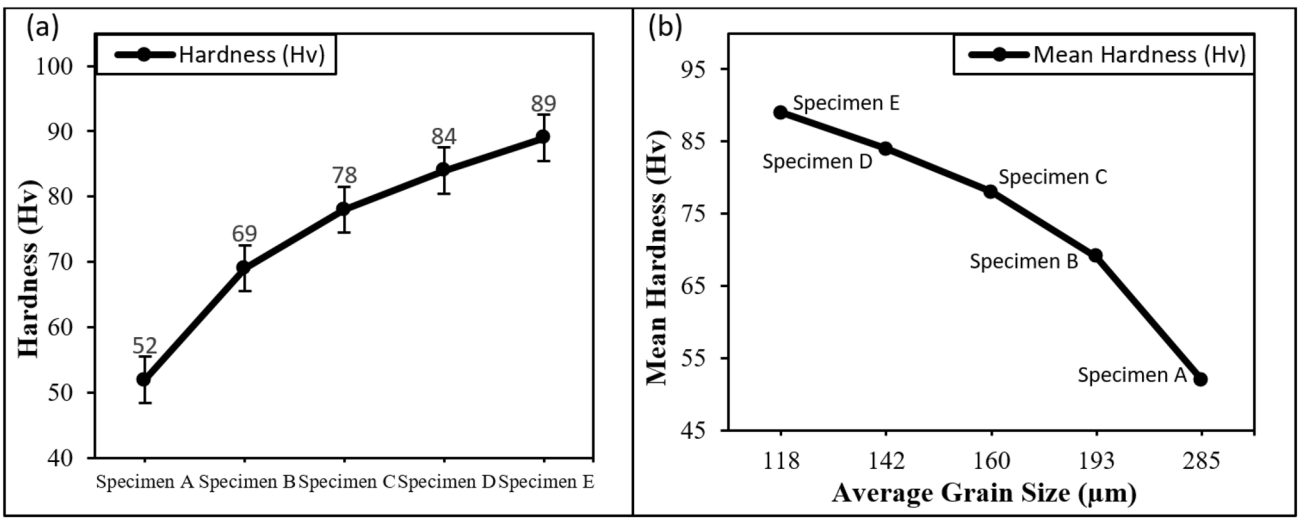

Fig. 8 **a** Hardness of fabricated specimens; **b** mean-hardness vs average grain size

de-bonding of α-Al and Si particles and leads to premature fracture. The porosity produced during the stir-casting also acts as the stress concentration sites and result premature fracture. Therefore, addition of the reinforcement results decrement in the percentage elongation of the fabricated composites [18, 29].

For explaining fracture behaviour of the tensile test specimens, SEM images were taken and are shown in Fig. 6. Dimples indicate ductile fracture for AA6061 (Fig. 6a). Gas porosities, coarse dendrites and large inter-dendritic shrinkage are clearly visible in the figure (Fig. 6a). Plastic slip bands arrangements also appear in the SEM images which generally occurs during the ductile fracture [30]. Grain refinement and uniform distribution of reinforcement delay the formation of micro-voids and prohibit voids interlocking which leads to ligament fracture and consequently strength enhancement. Cleavage facets pattern appear in the fractography of fabricated AMMC (Fig. 6b). During tensile test, some of reinforced particles are withdrawn from the matrix (Fig. 6c, d). In the presence of this withdrawn particle zone and brittle facets fracture pattern, ductility of the fabricated AMMCs gets reduced.

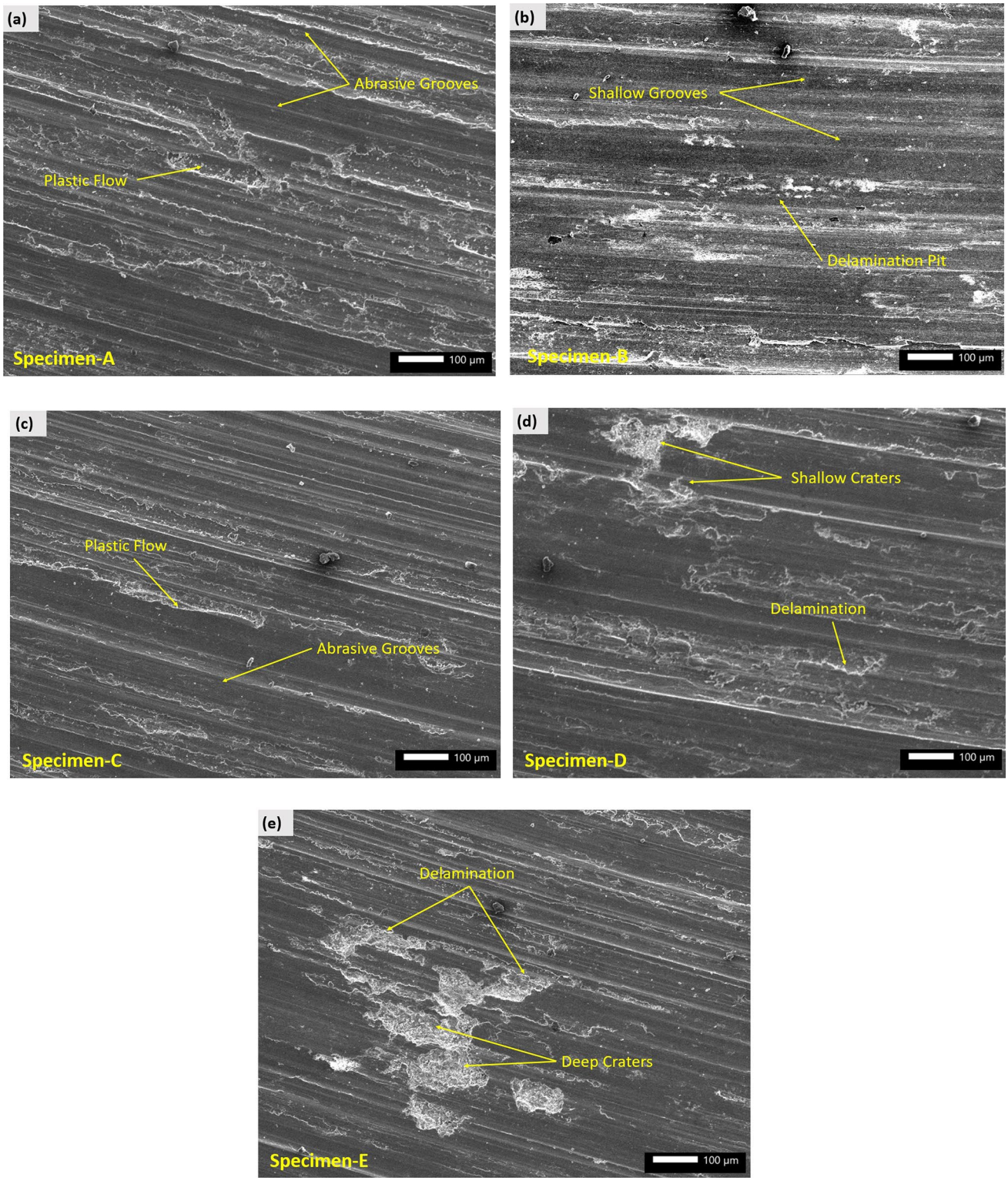

Fig. 9 SEM morphology of wear-out surfaces of fabricated specimens

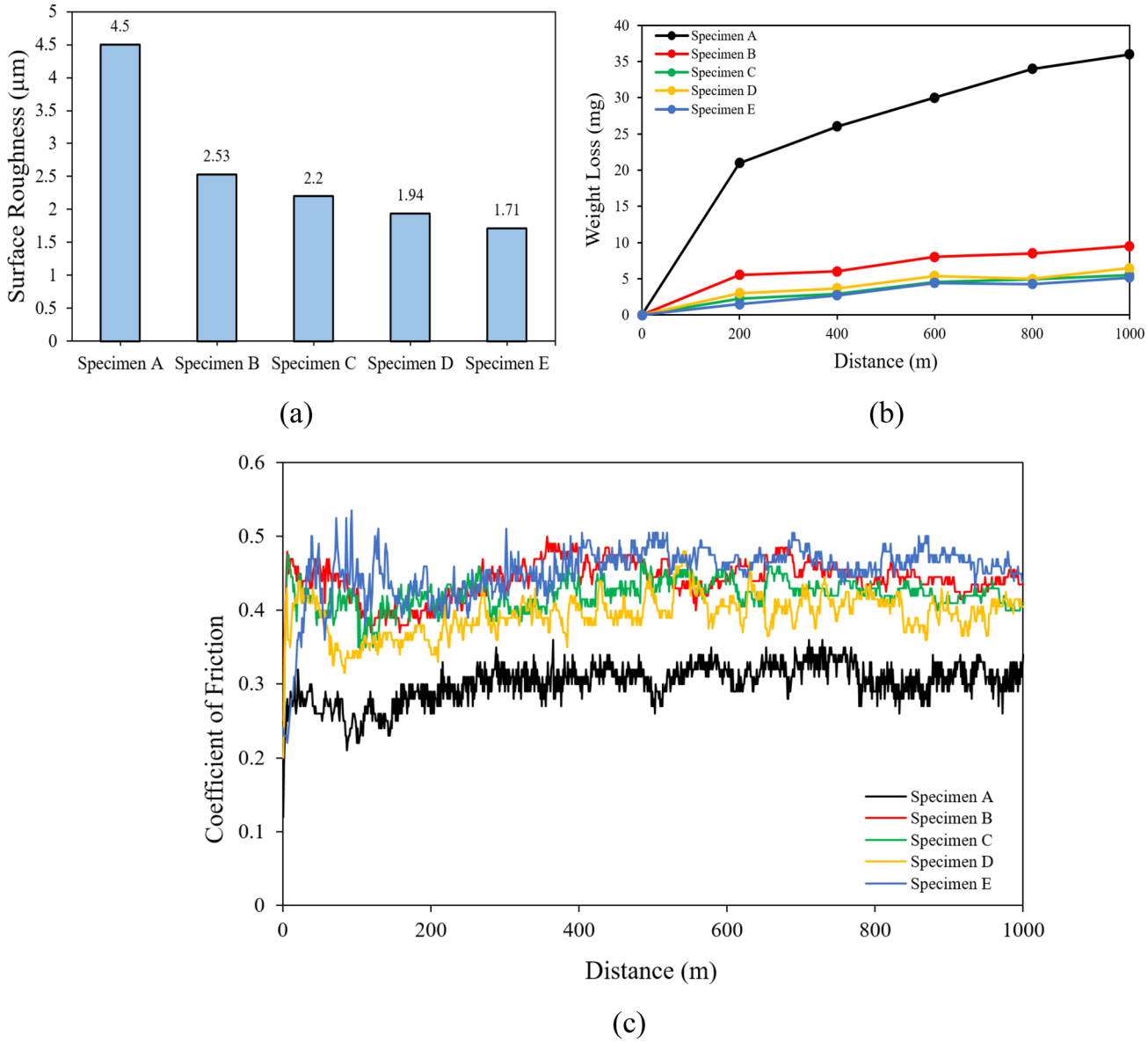

Fig. 10 **a** Surface roughness, **b** weight loss, **c** COF of worn-out surfaces

3.2.2 Compressive and Impact Strength

Figure 7 shows the compressive and impact strength of fabricated specimens. While applying crushing load, the deformation of the fabricated AMMC becomes complicated due to the reinforcement of hard particles. The measured compressive strength of Specimen-A was ~ 283 MPa; however, Specimen-B was ~ 317 MPa. Addition of NiTi also increases the compressive strength. When compared to Specimen-A & B, compressive strength of Specimen-E had increased by ~ 28.27 and ~ 14.51%, respectively (Fig. 7a). Stress produced in the course of compressive test was disseminated uniformly between matrix and reinforcement and causes the grain dislocations and improves the elasticity of the material. Applied load on the fabricated AMMCs gets efficiently transferred to the reinforcement due to clean matrix–particle interface. From Fig. 7b, it is found that impact strength of Specimen-A is greater than the Specimen-B. It is because of energy stored in stress concentration zone during plastic deformation is more in casted AA6061 when compared to the fabricated composite Specimen-B. Addition of small amount of NiTi (1wt%) significantly improved the impact strength of fabricated AMMC. Calculated impact strength of Specimen-C, D and E was ~ 18.3 J, ~ 18.9 J and ~ 19.0 J, respectively. This could be because of integration of hard and brittle particle bounds the rapid loading. Due to clean interface between matrix and the reinforcement, they also absorb the maximum energy before sample break. Compared

to the published literature, fabricated hybrid composite resulted in higher compressive and impact strength [11, 16].

3.2.3 Microhardness

Hardness of a material is defined as its ability to resist the localised permanent penetration, typically by indentation. Figure 8 shows the effect of reinforcement on the hardness of fabricated AMMC and linear increment in the hardness of composites can be detected. When compared to Specimen-A, Specimen-B has ~ 32.69% improvement in hardness. Addition of NiTi particles further improved the hardness by ~ 29% (69–89 Hv) for Specimen-E. Reinforcement $NiTi_p$ in Al-SiC/ZrO_2 results better microhardness, when compared to $NiTi_p$ reinforcement in Aluminium alloys [19].

Due to reinforcement, refinement of grains takes place and increases the strain field surrounding the matrix and reinforcement interface. It resists the depression in the material. Load transfer from the matrix to reinforcement also resists the indentation in material. In the fabricated AMMCs, grain size decreases as the reinforcement content increases. Lower grain size has higher number of grain boundaries in a specific area. These grain boundaries obstruct the movement of the dislocations, hence higher hardness.

3.3 Tribological Behaviour of Fabricated Specimens

Figures 9 and 10 represent the SEM of wear-out surface, surface roughness, weight-loss and coefficient of friction (COF) of wear-out samples, respectively. As NiTi wt% increases, surface roughness value of fabricated composites decreases (Fig. 10a).

SEM morphology of wear-out surface of Specimen-A shows some broken areas with patches and channels from abrasion (Fig. 9a). This indicates the tendency of Specimen-A to plastically deform when subjected to shearing of the irregularities of the another surface. Adding reinforcements to Specimen-A increases the COF value, but slightly decreases its variability due to increased hardness and decreased plasticity of the fabricated AMMCs. Therefore, a mild groove is observed in Specimen-B, indicating significantly reduced wear. However, significant pits caused by delamination have been observed in Specimen-B (Figs. 9b and 10b). Decreased thermal conductivity of the reinforcement caused the heat accumulation to the adjacent during sliding and forms delamination pits [31].

Higher hardness of the fabricated composites leads to the reduction in the abrasion; however, delamination was considerably increased. The R_a values of Specimen-A and Specimen-B demonstrate that in the case of composites, delamination pits were shallower than the abrasion grooves compared to Specimen-A. Increase in the hardness increases the resistance of the asperities to penetrate the surface, resulting in reduction in COF (Fig. 10c). It can also be seen that Specimen-C has far fewer wear grooves and lower R_a than Specimen-A and B. This indicates that asperities had less penetration and resulted in less wear loss (Fig. 10b).

Composite with 2wt%NiTi has lower COF and higher hardness. The reduction in grain size resulted in increased phonon scattering and consequent heat pile-up within the grain themselves. As a result, there was more adhesive interaction and delamination. Therefore, Specimen-D experienced greater wear loss than Specimen-C. COF of composite with 3wt%NiTi was higher than that of 2wt%NiTi. A small imbalance between peaks and valleys (excluding few regions) can be seen in Fig. 10c. It implies less abrasion grooves and increase in adhesion. The significant COF variation of 3wt%NiTi composites was caused by the increased adhesion force. Adhesive wear did not increase as much as abrasive wear, so the amount of wear decreased. When compared to Al–SiC–ZrO_2 composite, fabricated hybrid composite offers better wear performance [10, 15].

4 Conclusions

In the present work, NiTi/SiC/ZrO_2 reinforcement-based hybrid aluminium-MMCs were fabricated utilising liquid stir-casting for numerous industrial applications. The effect of NiTi wt% on microstructure, mechanical and tribological behaviour of Al/SiC/ZrO_2/NiTi-MMCs was studied. Based on investigation, following conclusions can be made:

- As-cast AA6061 has shown low strength, ductility and wear resistance due to the presence of porosity, coarse grains and α-Al dendrites.
- Addition of reinforcement improves the microstructure, mechanical and tribological behaviour of fabricated AMMCs.
- Addition of 2wt%NiTi results in 44.8% and 7.73% increment in tensile strength of fabricated MMC when compared to the AA6061 and Al/(SiC/ZrO_2)-MMC, respectively.
- Addition of 3wt%NiTi improves compressive strength, hardness and impact strength by 12.67, 28.98 and 18.01%, respectively, when compared to Al/(SiC + ZrO_2)-MMC.
- Addition of NiTi increases the COF due to increased adhesion, but decreases the wear loss and surface roughness of worn-out surface.

Acknowledgements Authors acknowledge the Department of Metallurgy and Materials Engineering, PEC Chandigarh for allowing usage of testing facilities.

Authors Contribution Saurabh Kumar Maurya and Chander Kant Susheel have designed the research, performed experiments, analysed

data and drafted the original research article. Alakesh Manna provided technical guidance and reviewed the manuscript.

Funding No funding was received for conducting this research. The authors declare they have no financial interests.

Declarations

Conflict of interests The authors report no competing interests to declare.

References

1. Eliasson J, and Sandstrom R, *Key Engineering Materials* **104** (1995) 3–36.
2. Dhanasekaran S, Sunilraj S, Ramya G, and Ravishankar S, *Transactions of the Indian Institute of Metals* **69** (2016) 699–703.
3. Kumar V, and Sharma V, *Particulate Science and Technology* **37** (2018) 770–780.
4. Mathur B, and Kumar P, *International Journal of Precision Technology* **10** (2021) 104–114.
5. Bandil K, Vashisth H, Kumar S, Verma L, and Gupta P, *Journal of Composite Materials*, 53 (2019) 4215–4223
6. Meena K L, Manna A, and Banwait S S, *American Journal of Mechanical Engineering* **1** (2013) 14–19.
7. Amouri K, Kazemi S, Momeni A, and Kazazi M, *Materials Science and Engineering: A* **674** (2016) 569–578.
8. Thirugnanasambandam A, Joy N, Mariadhas A, Raja KS, and Krishna BVS, In *AIP Conference Proceedings*, 2311 (2020), 080016
9. Rao T B, *Materials Science and Engineering:A* **805** (2021) 140553
10. Alizadeh A, Khayami A, Karamouz M, and Hajizamani M, *Ceramics International* **48** (2022) 179–189.
11. Pandiyarajan R, Maran P, Marimuthu S, and Ganesh K C, *Journal of Mechanical Science and Technology* **31** (2017) 4711–4717.
12. Kumar K R, Pridhar T, and Balaji V S, *Journal of Alloys and Compounds* **765** (2018) 171–179.
13. Kumar G V, Pramod R, Sekhar C G, Kumar G P, and Bhanumurthy T, *Heliyon* **5** (2019) 02858.
14. Khalili V, Heidarzadeh A, Moslemi S, and Fathyunes L, *Journal of Materials Research and Technology* **9** (2020) 15072–15086.
15. Arif S, Alam M T, Ansari A H, Siddiqui M A, and Mohsin M, *Materials Research Express* **4** (2017) 076511
16. Sekar K, Jayachandra G, and Aravindan S, *Materials Today: Proceedings* **5** (2018) 20268–20277.
17. Yadav S, Gangwar S, Yadav P C, Pathak V K, and Sahu S, *Surface Topography: Metrology and Properties* **9** (2021) 045022
18. Porter G A, Liaw P K, Tiegs T N, and Wu K H, *Jom* **52** (2000) 52–56.
19. Dixit M, Newkirk J W, and Mishra R S, *Scripta Materialia* **56** (2007) 541–544.
20. Thorat RR, Risanti DD, SanMartín, D, and VanDer Zwaag S, *Journal of Alloys and Compounds*, 477 (2009) 307–315
21. Ni D R, Wang J J, Zhou Z N, and Ma Z Y, *Journal of Alloys and Compounds* **586** (2014) 368–374.
22. Shanmugavel R, Mokkandi P, Jayamani M, Rajini N, and Thirumalaikumaran S, *Journal of Australian Ceramic Society*, 53 (2017) 177–185
23. Zhao L, Ding L, Soete J, Idrissi H, and Simar A, *Composites Part A: Applied Science and Manufacturing*, 126 (2019) 105617
24. ASTM E8, Standard test methods for tension testing of metallic materials. Annual book of ASTM standards, *ASTM International* (2001).
25. ASTM E9–19, Standard test methods of compression testing of metallic materials at room temperature", *ASTM international* (2009).
26. ASTM E23, Standard test methods for notched bar impact testing of metallic materials. E23–07a", *Pennsylvania, PA, USA* (2007).
27. Myriounis D P, Hasan S T, and Matikas T E, *Composite Interfaces* **15** (2008) 495–514.
28. Armstrong R W, *Acta Mechanica* **225** (2014) 1013–1028.
29. Kumar H, Prasad R, Kumar P, Tewari S P, and Singh J K, *Journal of Alloys and Compounds* **831** (2020) 154832
30. Sekar K, Allesu K, and Joseph M A, *Transactions of the Indian Institute of Metals* **68** (2015) 115–121.
31. Patel S K, Singh V P, and Kuriachen B, *Transactions of the Indian Institute of Metals* **72** (2019) 1765–1774.